

Conditional Image Retrieval

Mark Hamilton^{1 2}, Stephanie Fu¹, Mindren Lu¹, William T. Freeman¹³

¹ MIT ² Microsoft ³ Google
markth@mit.edu, fus@mit.edu, mdlu@mit.edu, billf@mit.edu

Abstract

This work introduces Conditional Image Retrieval (CIR) systems: IR methods that can efficiently specialize to specific subsets of images on the fly. These systems broaden the class of queries IR systems support, and eliminate the need for expensive re-fitting to specific subsets of data. Specifically, we adapt tree-based K-Nearest Neighbor (KNN) data-structures to the conditional setting by introducing additional inverted-index data-structures. This speeds conditional queries and does not slow queries without conditioning. We present two new datasets for evaluating the performance of CIR systems and evaluate a variety of design choices. As a motivating application, we present an algorithm that can explore shared semantic content between works of art of vastly different media and cultural origin. Finally, we demonstrate that CIR data-structures can identify Generative Adversarial Network (GAN) “blind spots”: areas where GANs fail to properly model the true data distribution.

1 Introduction

In many Image Retrieval (IR) applications, it is natural to limit the scope of the retrieval to a subset of images. For example, returning similar clothes by a certain brand, or similar artwork from a specific artist. Currently, it is a challenge for IR systems to restrict their attention to sub-collections of images on the fly. More specifically KNN data-structures, which are a core component of many IR systems, only support queries over the entire corpus. Currently, restricting retrieved images to a particular class or filter requires filtering the “unconditional” query results, or building a new KNN data-structure for each filter. The former approach is used in several production image search systems (DeGenova 2017; bin 2017), but can be costly if the filter is specific, or the query image is far from valid images. On the other hand, rebuilding the KNN data-structure on each subset of the data is costly and can result in 2^n data-structures, where n is the total number of images. To mitigate these issues, we introduce “conditional” variants of tree-based KNN methods that can efficiently and adaptively prune their structure to fit arbitrary conditional predicates. We evaluate the query-time performance of these methods compared to several baselines and

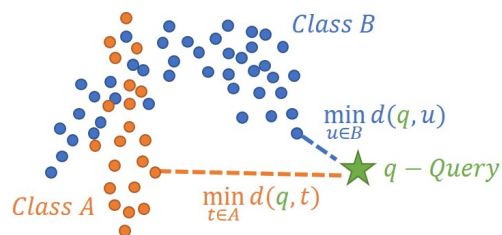


Figure 1: Conditional K-Nearest Neighbors for a query point, q , and distance, d , on a simple two class dataset.

introduce two new datasets to measure the semantic quality of these systems.

We apply CIR on the combined open-access collections of the the Metropolitan Museum of Art (Met 2019) and the Rijksmuseum (Rij 2019) to create a novel algorithm capable of identifying artistic connections across time, space, culture and media. Finally, we investigate the structure of conditional KNN trees to show that they can reveal areas of poor convergence and diversity (“blind spots”) in image based GANs. We summarize the contributions of this work as follows:

- We contribute a simple modification to existing KNN data-structures to allow users to efficiently filter resulting neighbors using arbitrary logical predicates, enabling efficient CIR
- We introduce two new datasets for evaluating CIR systems and use these datasets to evaluate various featurization strategies
- We use CIR to discover shared structure across genres, styles, artists, and media in the visual arts
- We use CIR data-structures to discover “blind spots” where GANs fail to match the true data

2 Background

IR systems aim to retrieve a list of relevant images that are related to a query image. “Relevance” in IR systems often refers to the “semantics” of the image such as its content, objects, or meaning. Many existing IR systems map images to “feature space” where distance better corresponds to relevance. In feature space, KNN can provide a ranked list of relevant images (Manning, Raghavan, and Schütze 2008).

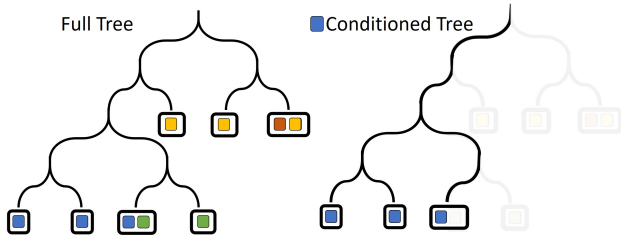


Figure 2: A schematic diagram of a full conditional search tree (Left). Colored blocks represent the existence of an image class labels within the leaf node. After conditioning on a particular class, one can prune nodes without any children satisfying the conditions. (Right)

Algorithm 1: Querying a CKNN Tree

input : A point, q , a condition, $\mathcal{S} \subseteq \mathcal{X}$, a tree, $root$, and an inverted index, I
output: Closest point, $p^* \in \mathcal{S}$, to q
 $validNodes \leftarrow \bigcup_{s \in \mathcal{S}} I(s)$; $p^* \leftarrow \text{null}$
def SearchNode(n) :
 if $n \in validNodes$ **then**
 if n is a leaf node **then**
 $p \leftarrow \text{closest point in } \mathcal{S}$
 if $d(p, q) < d(p^*, q)$ **then**
 $p^* \leftarrow p$
 else
 $potentials \leftarrow \text{children of } n \text{ which could hold a closer point}$
 for $child$ in $potentials$ **do**
 SearchNode($child$)
 SearchNode($root$) ; **return** p^*

Good features and distance metrics aim to align with our intuitive senses of similarity between data (Yamins et al. 2014) and show invariance to certain forms of noise (Gordo et al. 2016). In this work we leverage features from intermediate layers of deep supervised models, which perform well in a variety of contexts and are ubiquitous throughout the literature. Nevertheless, our methods could apply to any features found in the literature including those 3 from collaborative filtering, text, sound, and tabular data.

There are a wide variety of KNN algorithms, each with their own strengths and weaknesses. Typically, these methods are either tree-based, graph-based, or hash-based (Aumüller, Bernhardsson, and Faithfull 2018). Tree-based methods partition target points into hierarchical subsets based on their spatial geometry and include techniques such as the KD Tree (Bentley 1975), PCA Tree (Bachrach et al. 2014), Ball Tree (Omohundro 1989), some inverted index approaches (Baranchuk, Babenko, and Malkov 2018), and tree ensemble approaches (Yan et al. 2019). Some tree-based data-structures allow exact search with formal guarantees on their performance (Dasgupta and Freund 2008). Graph-based methods rely on greedily traversing an approximate KNN graph of the data, and have gained popularity due to their superior performance in the approximate NN do-

Component	Space Efficiency	Measured
Data	$\mathcal{O}(n \times d)$	380 MB
Tree	$\mathcal{O}((2n/l) \times d)$	7.6 MB
Conditional Index	$\mathcal{O}(c \times 2n/l)$.02 MB

Table 1: Space efficiency of a binary CKNN Tree with number of points, n , dimensionality, d , leaf size l , and number of classes in the index, c . Measured results are for a tree built on MNIST dataset: $n = 60000$, $d = 784$, $l = 100$, $c = 10$.

main (Aumüller, Bernhardsson, and Faithfull 2018; Johnson, Douze, and Jégou 2019). There are numerous hash-based approaches in the literature and (Wang et al. 2014) provides a systematic overview. To our knowledge, neither graph nor hash-based retrieval methods can guarantee finding the nearest neighbor deterministically. However, fast approximate search is often sufficient for many applications. In our work we focus on tree-based methods because it is unclear how to create an analogous method for graph-based data-structures. Nevertheless, tree based methods are widely used, especially when exact results are required.

3 Conditional Nearest Neighbors

The Conditional K-Nearest Neighbors (CKNN) of a query point, q , are the the k closest points with respect to the distance function, d that satisfy a given logical predicate (condition), \mathcal{S} . We represent this condition as a subset of the full corpus of points, \mathcal{X} :

$$CKNN(q, \mathcal{S} \subseteq \mathcal{X}) = \underset{t \in \mathcal{S}}{\operatorname{argmin}} d(q, t)$$

When the conditioner, \mathcal{S} , equals the full space, \mathcal{X} , we recover the standard KNN definition. Figure 1 shows a visualization of CKNN for a two dimensional dataset with two classes. The goal of this work is to show that, for a broad class of KNN data-structures, it is possible to perform “predicate push-down” (Hellerstein and Stonebraker 1993; Levy, Mumick, and Sagiv 1994) and move condition requirements and logical predicates into the KNN data-structure to improve search speed. We stress that this work does **not** aim to make the fastest KNN algorithm, or to exhaustively implement predicate push-down in all KNN methods. Our aim is to show that conditioning a KNN data-structure on the fly is possible, has small overhead, yields new tools for image analysis, and can improve performance when added to a commonly used implementation (Pedregosa et al. 2011) of the Ball tree and KD tree data-structures.

To create an efficient CIR system we propose specializing an existing KNN data-structure trained on a corpora of points \mathcal{X} to a particular subset of points, $\mathcal{S} \subseteq \mathcal{X}$. To specialize tree based KNN methods to particular subsets, we can filter or “prune” irrelevant data in the leaves of the tree and inner nodes without relevant children. Figure 2 diagrams a simple pruning operation where nodes are pruned if they do not contain points that satisfy the conditioning predicate. To prune nodes quickly and efficiently we introduce an inverted index (Knuth 1997), I , that maps points, $x \in \mathcal{X}$ to the collection of their dominating nodes,

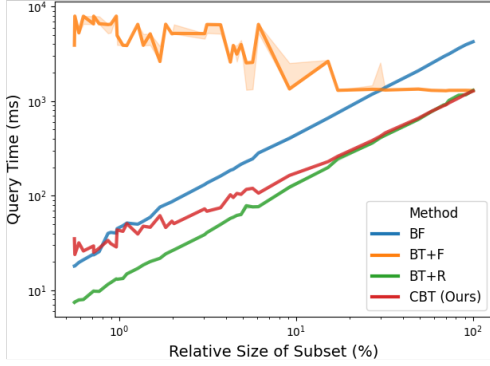


Figure 3: Query time of CKNN approaches. Our approach, CBT, achieves query performance of a tree recreated specifically for each query without the expensive re-creation cost, and does not perform poorly with small conditions like query-then-filter approaches (BT+F). Please see Section 3.2 for method details.

Dataset	CKNN Method				
	BF	BT+F	LPQ+F	BT+R	CBT
FMNIST	8	65	13	6 + 3k	8
MNIST	7	58	10	6 + 3k	9
Glove-25	29	160	122	6 + 7k	25
Glove-50	41	266	132	23 + 11k	37
Glove-100	66	477	176	40 + 17k	64
Glove-200	117	1306	310	52 + 32k	80
NYT	30	137	29	12 + 8k	21
SIFT	70	254	229	24 + 20k	42

Table 2: Query times (ms) of Conditional KNN methods across several benchmarking datasets from (Aumüller, Bernhardsson, and Faithfull 2018). Our conditional method, CBT, outperforms other approaches including those most commonly used in production search engines, LPQ+F. Please see the Section 3.2 for method details.

$I(x) = \{n : x \text{ below node } n\}$. We can form the union of dominating nodes, as shown in the first line of Algorithm 1, to compute the subset of nodes that remain after pruning. One can quickly prune nodes during traversal by checking node membership in this set. Furthermore, this set can be cached and shared between queries with the same conditioner. Leaf node points can be pruned through direct evaluation of the predicate. For scenarios where the predicates have additional structure, such as representing class labels, one can define a smaller class-based inverted index, $I_{class}(c)$ which maps a class label, c , to the set of dominating nodes. For these predicates, union and intersection operators commute through the class-based inverted index:

$$\begin{aligned} I(\mathcal{S}_a \cap \mathcal{S}_b) &= I_{class}(a) \cap I_{class}(b) \\ I(\mathcal{S}_a \cup \mathcal{S}_b) &= I_{class}(a) \cup I_{class}(b) \end{aligned} \quad (1)$$

where \mathcal{S}_a is the subset of points with label a . This principle speeds a broad class of queries and accelerates document

retrieval frameworks like Elastic Search (Gormley and Tong 2015) and its backbone, Lucene (McCandless et al. 2010). We stress that our approach is more nuanced than simply using both Lucene and a KNN retrieval data-structure. In particular, we use a Lucene-style system to index subtrees of an underlying KNN data-structure to allow for on-the-fly KNN data-structure pruning. This approach can apply to a wide variety of KNN trees independent of how the tree splits points (Ball, Hyperplane, Cluster), the branching factor, and the topology of the tree. It also applies to ensembles of trees and to multi-probe LSH methods by pruning hash buckets.

3.1 Implementation

We implement predicate push-down for the existing Ball Tree and KD tree implementations in the popular SciKit-learn framework (Pedregosa et al. 2011). Our implementation supports exact retrieval with several metrics, OpenMP parallelization, and Cython acceleration. We also provide accelerations such as dense bit-array set operations, and caching node subsets on repeated conditioner queries. Finally, we contribute a Spark based implementation of a Conditional Ball tree to Microsoft ML for Apache Spark (Hamilton et al. 2018a,b) for large-scale, elastic, and distributed queries across a wide variety of databases and formats.

3.2 Performance

To analyze the speed of conditional KNN approaches we compare our conditional approach (CBT) with a vectorized brute force strategy (BF), remaking the KNN data-structure on the fly (+R), and query-then-filter (+F) baselines. Because these approaches are largely KNN-datastructure agnostic, we use the Ball Tree (BT) across these methods to standardize comparisons and refer to Table 4 of the Appendix for results with KD trees. We also compare against Locally Optimized Product Quantization with filtering (LOPQ+F) (Kalantidis and Avrithis 2014) because several modern visual search engines such as Flickr (Melina 2017), Bing (bin 2017), and Wayfair (DeGenova 2017) leverage this approach. We note that LOPQ could also benefit from our conditional index, but we have used the query-then-filter strategy to reflect current systems.

In Table 2 we evaluate our approach against several baseline methods and established benchmarking datasets (Aumüller, Bernhardsson, and Faithfull 2018). We query datasets with random conditions (10% of points) and average query times across all conditions. Our results show that conditional data-structures approach the speed of predicate-specific data-structures but do not incur a large cost to re-make the data-structure for each query. Furthermore, conditional approaches are significantly faster than post-query filtering, as the latter can require a very large k to yield a point that satisfies the condition. We note that our approach beats a vectorized brute force strategy in most cases, and that a conditional method’s performance depends strongly on the performance of the underlying unconditional method. It is known that the Ball Tree performs better in lower dimensions as shown in Table 12 of the appendix. In Table 5 of the Appendix we also include results on conditions with spatial locality, such as clusters and class labels. Local conditions

Dataset	Metric	Featurization Method								
		RN50	RN101	MN	SN	DN	RNext	dlv3101	MRCNN	Random
CA	@1	.50	.51	.55	.44	.59	.46	.37	.45	.0002
	@10	.70	.68	.71	.62	.76	.65	.55	.63	.002
CF	@1	.41	.37	.39	.44	.43	.38	.33	.44	.016
	@10	.77	.76	.76	.80	.79	.76	.73	.79	.16
FEI	@1	.80	.84	.85	.79	.87	.86	.72	.78	.005
	@10	.94	.93	.94	.89	.95	.94	.86	.92	.05

Table 3: Performance of CIR (Accuracy @ N) on content recovery across style variations for both the ConditionalFont (CF) and ConditionalArt (CA) datasets using a variety of features from pre-trained networks. Results show CIR retrieves the same content image across different styles. For full details on experimental conditions see Section 7

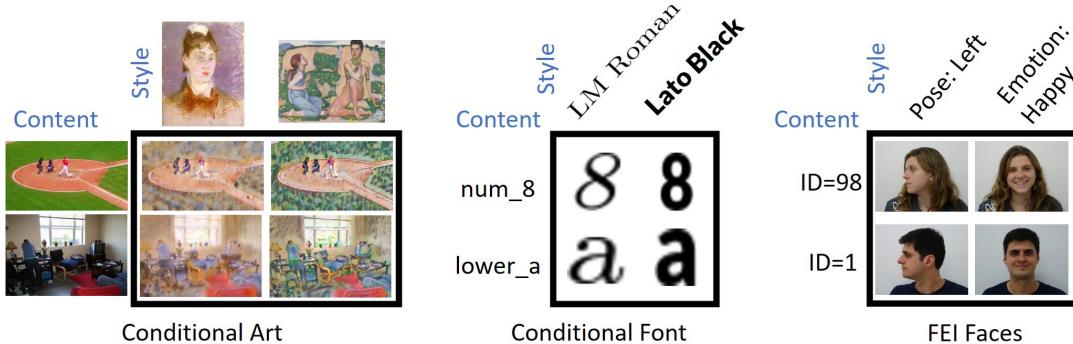


Figure 4: Representative samples from the ConditionalArt dataset (left), ConditionalFont dataset (middle), and FEI Face dataset (right). CIR systems conditioned on style should retrieve images of the same content.

improve conditional tree performance by increasing pruning but dramatically harm query-then-filter style approaches (BT+R and LOPQ+R) because many irrelevant points can sit between the query point and the subset of points that satisfies the conditions.

To understand the effects of predicate size, we measure query speed on on 488k Resnet50-featurized images ($dim = 2048$) from the combined MET and Rijksmuseum open-access collections with a randomly chosen test set ($n = 1000$). We condition on artwork media, culture, and several combinations of these to create a variety of condition sizes. In Figure 3, we compare the performance of our baselines as a function of conditioner size. We note that conditional trees approach the performance of dedicated trees for most of the predicates tested, but without the expensive cost of recreating the tree (Creation time not included in Figure 3). Furthermore, we note that the approach dominates brute force search up to 1% of the data for Ball trees. We also observe the expected deterioration in performance of the query-then-filter strategy as conditioners become more specific. For implementation, experimentation, environment, and computing details please see Section 7.

We found that conditioning a KNN data-structure does not introduce significant space and time overhead. In Table 1 we show that the space overhead of our conditional index is small compared to the data held within the tree, and the tree itself. We also found that that cost of creating the conditional index is orders of magnitude smaller than building the underlying tree. In the scenario when $\mathcal{S} = \mathcal{X}$, we can directly

compare the performance of conditional and unconditional data-structures. Figure 11 and Table 6 in the Appendix show query time distributions for conditional and unconditional variants of the KD and Ball Tree. These experiments show that checking the node subset before each branch traversal adds negligible overhead. CKNN performance is dominated by that of the underlying unconditional KNN data-structure which is often data-dependant.

4 Discovering Shared Structure in Visual Art

One application of CIR is to reveal cultural connections in the visual arts. More specifically, CIR on the combined Met and Rijksmuseum collections finds striking connections between art from different histories and mediums. These matches can highlight cultural exchange and shared inspiration such as the Dutch Double Face Banyan (left) and the Chinese ceramic figurine (top row second from left) of Figure 5. It’s possible to trace these to the flow of porcelain and iconography from Chinese to Dutch markets during the 16th-20th centuries (Le Corbeiller 1974; Volker 1954). We hope CIR can help art-historians and inspire the public to explore new artistic traditions. To this end, we introduce a live and interactive website to explore CIR in the visual arts in Section A of the Appendix. We also provide additional matches in Section G of the Appendix.

To create this method, we leverage features from the penultimate layer of ResNet50 (He et al. 2016) trained on ImageNet (Deng et al. 2009) which has been shown to capture many aspects of image semantics such as texture, color,

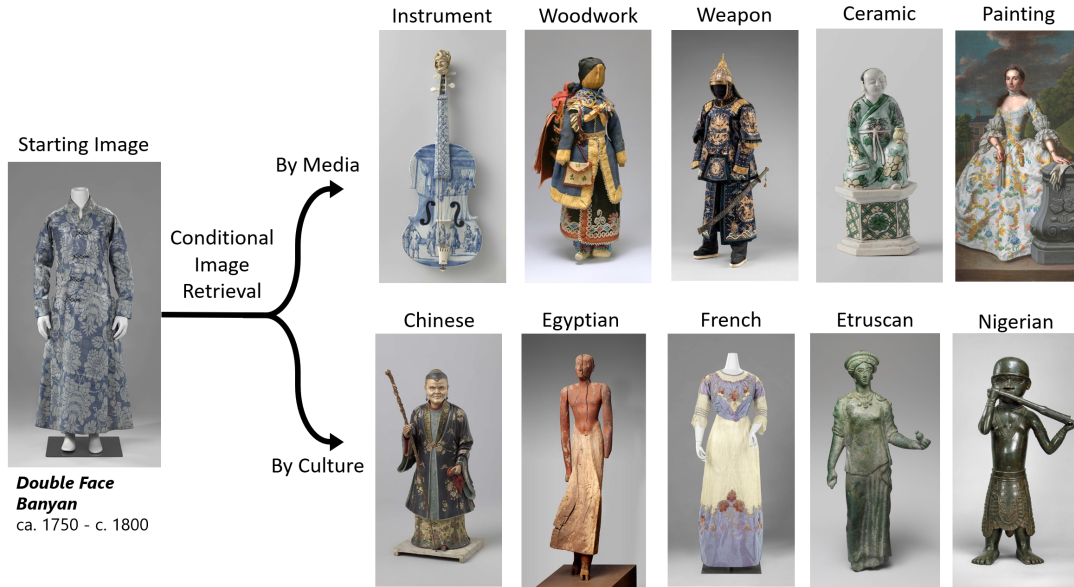


Figure 5: Conditional image retrieval results on artworks from the Metropolitan Museum of Art and Rijksmuseum using media (top row text) and culture (bottom row text) as conditioners.

content, and pose (Olah, Mordvintsev, and Schubert 2017). In this work we use “content” features from ResNet50. Alternatively one could use “style” based features from methods like AdaIN (Huang and Belongie 2017), or the Gram Matrix of (Gatys, Ecker, and Bethge 2016) to create a CIR system that retrieves images by “style” with an approximate invariance to image content.

4.1 Evaluation by Non-parametric Style Transfer

The performance of a CIR system is largely dependent on the choice of image features. We measure the quality of different featurization strategies for CIR by retrieving similar-content images across different “stylizations”. More specifically, if the conditioning information represents the image “style” and the features represent the “content”, CIR should find an image with the same content, but constrained to the style of the conditioner, such as “Ceramic” or “Egyptian” in Figure 5. Through this lens, CIR systems can act as “non-parametric” style transfer systems. This approach finds analogous images within an existing corpora and differs from existing style transfer and visual analogy methods in the literature that generate new images (Huang and Belongie 2017; Gatys, Ecker, and Bethge 2016)

To evaluate CIR’s semantic performance we introduce two datasets with known style and content annotations: the ConditionalFont and ConditionalArt datasets. The ConditionalFont dataset contains 15687 32×32 greyscale images of 63 ASCII characters (content) across 249 fonts (style). The ConditionalArt dataset contains 100000 color images of varying resolution formed by stylizing 5000 content images from the MS COCO (Lin et al. 2014) dataset with 200 style images from the WikiArt dataset (Nichol 2016) using a Adaptive Instance Normalization (Huang and Belongie 2017). Although this dataset is “synthetic”, (Jing et al.

2019) show that neural style transfer methods align with human intuition. We also evaluate our approach on the FEI Faces database which contains 2800 high resolution faces of 200 participants across 14 poses, emotions, and lighting conditions. We show representative samples from each dataset in Figure 4. With these datasets it’s possible to measure how CIR features, metrics, and query strategies affect CIR’s ability to match content across styles. To measure retrieval accuracy, we sampled 10000 random query images. For each random query image, we use CIR to retrieve the query image’s KNNs conditioned on a random style. We then check whether any retrieved images have the same content as the original query image. In Table 3, we explore how the choice of featurization algorithm affects CIR systems. All methods outperform the random baseline of Table 3, indicating that they are implicitly performing non-parametric content-style transfer. DenseNet (DN) (Iandola et al. 2014) and Squeezenet (SN) (Iandola et al. 2016) tend to perform well across all datasets.

5 Limitations

This work does not aim to create the fastest KNN algorithm, but rather presents a broadly applicable conditioning scheme that’s simple, effective, and yields fruitful applications. We note that KNN retrieval chooses particular items significantly more than others, due to effects such as the “hubness problem” and we direct readers to (Dinu, Lazari-dou, and Baroni 2014) for possible solutions. We identify some lower dimensional failure cases that do not correspond to those mentioned by Dinu et al and explore this further in Section B of the Appendix. Our approach does not modify the KNN construction, simply prunes it afterwards. This is clearly not the most efficient solution when conditioner sizes are small, but it is orders of magnitude faster than recreat-

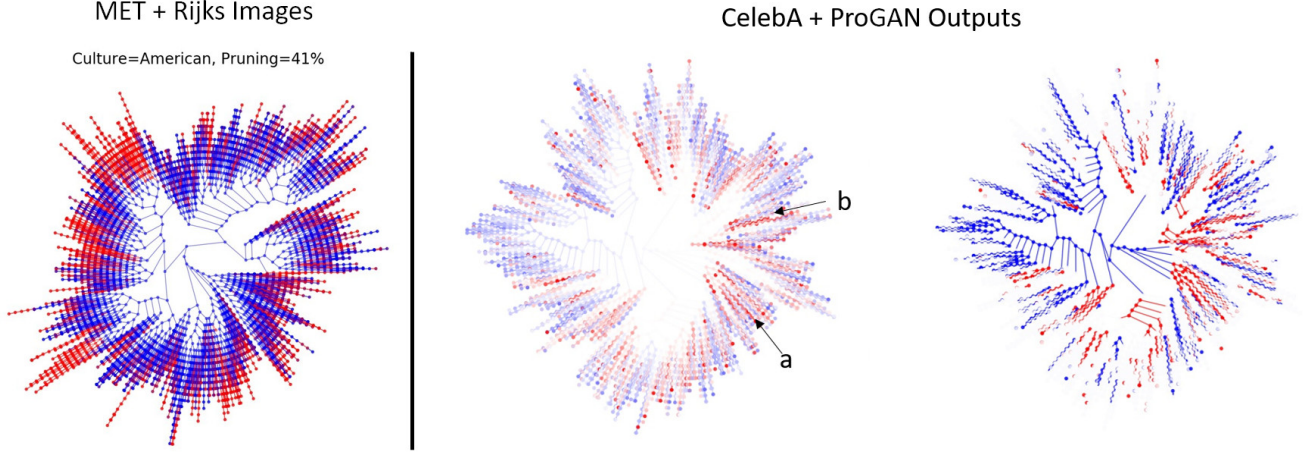


Figure 6: (Left): Visualization of the American culture class within MET+Rijks CBT. Points represent CBT nodes. Red nodes contain no American artworks and are pruned during retrieval. The pruning rate (41%) is significantly higher than random chance (12%) suggesting the class is spatially localized. (Middle and Right): Visualization of CBT on ProGAN outputs and CelebA HQ images. (Middle): Nodes colored by RCD where blue nodes represent nodes with higher than average representation by the GAN. Nodes *a* and *b* are labelled, and samples from these nodes are shown in 7. (Right): Nodes colored by statistically significant deviations of RCD from 1 ($p < 0.01$) show widespread differences between GAN outputs and true data.

ing the tree. We also note that the performance of any conditional KNN tree is dominated by the underlying unconditional KNN tree, which often perform better on datasets with smaller intrinsic dimension. We illustrate this behavior in Figure 12 of the Appendix.

6 Discovering “Blind Spots” in GANs

Efficient high-dimensional KNN search data-structures need to robustly partition the data based on its variance and geometry. Several recent tree-based KNN data-structures use unsupervised learning methods like hierarchical clustering (Wang 2011) and slicing along PCA directions (Bachrach et al. 2014). In this light, KNN data-structures model of the hierarchical topology of the data and we can use this to study the “heterogeneity” of conditioning information relative to the full dataset. In Figure 6, we show that conditioners such as American Art in the MET and Rijks collections exhibit significant locality (41% node pruning) in the Conditional Ball Tree when compared to an equivalently sized random condition (12% node pruning). To quantify this, we introduce a simple and interpretable statistic, the Relative Conditioner Density (RCD), to measure the degree of over and under representation of a class c with corresponding subset $\mathcal{S}_c \subseteq \mathcal{X}$, at node n in the KNN tree:

$$RCD(n, c) = \frac{|n \cap \mathcal{S}_c|}{|n|} \frac{|\mathcal{X}|}{|\mathcal{S}_c|} \quad (2)$$

Here, $|n|$ represents the number of data below node n in the tree. The RCD measures how much a node’s empirical distribution of labels differs from the global statistics. $RCD > 1$ occurs when the node over-represents class c , and $RCD < 1$ occurs when the node under-represents a class, c . We apply this statistic to understand how samples

from generative models, such as image-based GANs, differ from true data. In particular, one can form a conditional tree containing true data and generated samples, each with their own classes, c_t and c_g respectively. In this context, nodes with $RCD(\cdot, c_g) \ll 1$ are regions of space where the network under-represents the real dataset. In Figure 6, we form a Conditional Ball Tree for samples from a trained Progressive GAN (Karras et al. 2017) and the training dataset: CelebA HQ (Liu et al. 2015). Coloring the nodes by RCD reveals a considerable amount of statistically significant structural differences between the two distributions. By simply thresholding the RCD (< 0.6), we find types of images that GANs struggle to reproduce. We show samples from two low-RCD nodes in Figure 7 and also note their location in Figure 6. From a visual inspection of the real samples below this node, one can see that Progressive GAN struggles to generate realistic images of brimmed hats as well as microphones. Though we do not focus this work on thoroughly investigating issues of diversity in GANs, this suggests GANs have difficulty representing data that is not in the majority. This aligns with the findings of (Bau et al. 2019), without requiring GAN inversion, additional object detection labels, or a semantic segmentation ontology.

7 Experimental Details

We perform all timed comparisons in Table 2 and Table 6 of the Appendix, on an Azure NV24 Virtual Machine running Ubuntu 16.04, Python 3.7, and scikit-learn v0.22.2 (Pedregosa et al. 2011). We use scikit-learn for Ball Tree and KD Tree implementations and use numpy v1.18.1 for brute force implementations. We use the open source “lopq” library for Locally Optimized Product Quantization experiments. For query-then-filter strategies we first retrieve 50 points, then increase geometrically (x5) if



Figure 7: Samples from two statistically significant nodes from Figure 6. Images are randomly chosen and representative of those found at the node. Almost every real image in Node a contains microphones whereas no GAN generated outputs could create a microphone. Node b shows a clear bias towards brimmed hats, and the GAN samples contain significant visual artifacts.

the query yields no valid matches. For performance tests we use the FMNIST, MNIST, GLOVE, NYT, and SIFT datasets from (Aumüller, Bernhardsson, and Faithfull 2018). To form image features for Table 3 we use trained networks from torchvision v0.6 (Marcel and Rodriguez 2010). In particular, we use ResNet50 (RN50) (He et al. 2016), ResNet101 (RN101), MobileNetV2 (MN) (Sandler et al. 2018), SqueezeNet (SN) (Iandola et al. 2016), DenseNet (DN) (Iandola et al. 2014), ResNeXt (RNext) (Xie et al. 2016), DeepLabV3 ResNet101 (dlv3101) (Chen et al. 2017), and Mask R-CNN (MRCNN) (He et al. 2017). Features are taken from the penultimate layer of the backbone, and the matches of Table 3 are computed with respect to cosine distance. We use trained a Progressive GAN from the open-source Tensorflow implementation accompanying (Karras et al. 2017).

8 Related Work

Image retrieval and nearest neighbor methods have been thoroughly studied in the literature, and there are many directions for future study. There are several survey works on KNN retrieval, but they only mention unconditional varieties (Bhatia et al. 2010; Wang et al. 2014). (Marchiori 2009) has studied the mathematical properties of conditional nearest neighbor retrieval for large margin classification, but works primarily with graph based methods as opposed to trees. They do not apply this to modern deep features and do not aim to improve query speed. There are a wide variety of featurization strategies for IR systems. Gordo et. al (Gordo et al. 2016) learn features optimized for IR. Siamese networks such as FaceNet embed data using tuples of two data and a similarity score and preserving this similarity in the embedding (Koch, Zemel, and Salakhutdinov 2015; Schroff, Kalenichenko, and Philbin 2015). These methods do not perform conditional retrieval, and features from these methods could be used to improve CIR systems. Conditional Similarity Networks augment tuple embedding approaches with the ability to handle different notions of similarity with different embedding dimensions (Veit, Belongie, and Karaletsos

2016). This models conditions as similarities, but does not generically restrict the search space of retrieved images to match a user’s query. These features have potential to yield neighbor trees that, when pruned, have a similar structure and performance to dedicated trees. Sketch-based IR uses line-drawings as query-images, but does not aim to restrict the set of candidate images generically (Lu et al. 2018). Style transfer (Jing et al. 2017) and visual analogies (Liao et al. 2017) yield results similar to our art exploration tool, but generate the analogous images rather than retrieve them from an existing corpus. (Traina, Trains, and de Figueiredo 2004) split IR systems into conditional subsystems, but do not tackle generic conditioners or provide experimental evaluation. (Plummer et al. 2018) create an IR system conditioned on text input, but do not address the problem of generically filtering results. (Gao et al. 2020) and (Liao et al. 2018) respectively learn and use a hierarchy of concepts concurrently with IR features, which could be a compelling way to *learn* useful conditions for an Conditional IR system.

9 Conclusion

We have presented and evaluated new methods for efficient conditional image retrieval. We provided simple and generic ways to modify broad classes of KNN architectures to support arbitrary conditional queries on the fly. These queries can shed light on hidden commonalities between corpora, improve result diversity, and tailor results to fit a user’s specifications. We demonstrated that this approach speeds conditional queries and approaches optimal results without adding overhead to the unconditional model. We showed that conditional IR can help reveal shared visual content across seemingly disparate artistic cultures and media. We introduced two new datasets, ConditionalFont and ConditionalArt, to quantitatively evaluate conditional IR and systematically explore the effect of different featurization strategies. Lastly, we explored the topology of CKNN data-structures to identify several “blind spots” in the ProGAN network trained on CelebA HQ.

References

2017. Beyond text queries: Searching with Bing Visual Search. URL <https://blogs.bing.com/search-quality-insights/2017-06/beyond-text-queries-searching-with-bing-visual-search>.
2019. The Metropolitan Museum of Art Open Access CSV. URL <https://github.com/metmuseum/openaccess>.
2019. The Rijksmuseum Open Access API. URL <https://data.rijksmuseum.nl/>.
- Aumüller, M.; Bernhardtsson, E.; and Faithfull, A. J. 2018. ANN-Benchmarks: A Benchmarking Tool for Approximate Nearest Neighbor Algorithms. *CoRR* abs/1807.05614. URL <http://arxiv.org/abs/1807.05614>.
- Bachrach, Y.; Finkelstein, Y.; Gilad-Bachrach, R.; Katzir, L.; Koenigstein, N.; Nice, N.; and Paquet, U. 2014. Speeding up the xbox recommender system using a euclidean transformation for inner-product spaces. In *Proceedings of the 8th ACM Conference on Recommender systems*, 257–264.
- Baranchuk, D.; Babenko, A.; and Malkov, Y. 2018. Revisiting the Inverted Indices for Billion-Scale Approximate Nearest Neighbors. *CoRR* abs/1802.02422. URL <http://arxiv.org/abs/1802.02422>.
- Bau, D.; Zhu, J.-Y.; Wulff, J.; Peebles, W.; Strobel, H.; Zhou, B.; and Torralba, A. 2019. Seeing What a GAN Cannot Generate.
- Bentley, J. L. 1975. Multidimensional binary search trees used for associative searching. *Communications of the ACM* 18(9): 509–517.
- Bhatia, N.; et al. 2010. Survey of nearest neighbor techniques. *arXiv preprint arXiv:1007.0085*.
- Chen, L.; Papandreou, G.; Schroff, F.; and Adam, H. 2017. Re-thinking Atrous Convolution for Semantic Image Segmentation. *CoRR* abs/1706.05587. URL <http://arxiv.org/abs/1706.05587>.
- Dasgupta, S.; and Freund, Y. 2008. Random projection trees and low dimensional manifolds. In *Proceedings of the fortieth annual ACM symposium on Theory of computing*, 537–546.
- DeGenova, V. 2017. Recommending Visually Similar Products Using Content Based Features. URL <https://tech.wayfair.com/data-science/2017/12/recommending-visually-similar-products-using-content-based-features/>.
- Deng, J.; Dong, W.; Socher, R.; Li, L.-J.; Li, K.; and Fei-Fei, L. 2009. Imagenet: A large-scale hierarchical image database. In *2009 IEEE conference on computer vision and pattern recognition*, 248–255. Ieee.
- Dinu, G.; Lazaridou, A.; and Baroni, M. 2014. Improving zero-shot learning by mitigating the hubness problem. *arXiv preprint arXiv:1412.6568*.
- Fedosejev, A. 2015. *React.js essentials*. Packt Publishing Ltd.
- Gao, X.; Mu, T.; Goulermas, J. Y.; Thiyaalingam, J.; and Wang, M. 2020. An Interpretable Deep Architecture for Similarity Learning Built Upon Hierarchical Concepts. *IEEE Transactions on Image Processing* 29: 3911–3926.
- Gatys, L. A.; Ecker, A. S.; and Bethge, M. 2016. Image style transfer using convolutional neural networks. In *Proceedings of the IEEE conference on computer vision and pattern recognition*, 2414–2423.
- Gordo, A.; Almazán, J.; Revaud, J.; and Larlus, D. 2016. Deep image retrieval: Learning global representations for image search. In *European conference on computer vision*, 241–257. Springer.
- Gormley, C.; and Tong, Z. 2015. *Elasticsearch: the definitive guide: a distributed real-time search and analytics engine*. ” O’Reilly Media, Inc.”.
- Grave, E.; Joulin, A.; and Berthet, Q. 2018. Unsupervised Alignment of Embeddings with Wasserstein Procrustes.
- Hamilton, M.; Raghunathan, S.; Annavaajhala, A.; Kirsanov, D.; de Leon, E.; Barzilay, E.; Mاتيach, I.; Davison, J.; Busch, M.; Opreescu, M.; et al. 2018a. Flexible and scalable deep learning with MMLSpark. *arXiv preprint arXiv:1804.04031*.
- Hamilton, M.; Raghunathan, S.; Mاتيach, I.; Schonhoffer, A.; Raman, A.; Barzilay, E.; Rajendran, K.; Banda, D.; Hong, C. J.; Knoertzer, M.; et al. 2018b. MMLSpark: Unifying Machine Learning Ecosystems at Massive Scales. *arXiv preprint arXiv:1810.08744*.
- He, K.; Gkioxari, G.; Dollár, P.; and Girshick, R. B. 2017. Mask R-CNN. *CoRR* abs/1703.06870. URL <http://arxiv.org/abs/1703.06870>.
- He, K.; Zhang, X.; Ren, S.; and Sun, J. 2016. Identity mappings in deep residual networks. In *European conference on computer vision*, 630–645. Springer.
- Hellerstein, J. M.; and Stonebraker, M. 1993. Predicate migration: Optimizing queries with expensive predicates. In *Proceedings of the 1993 ACM SIGMOD international conference on Management of data*, 267–276.
- Huang, X.; and Belongie, S. 2017. Arbitrary style transfer in real-time with adaptive instance normalization. In *Proceedings of the IEEE International Conference on Computer Vision*, 1501–1510.
- Iandola, F.; Moskewicz, M.; Karayev, S.; Girshick, R.; Darrell, T.; and Keutner, K. 2014. Densenet: Implementing efficient convnet descriptor pyramids. *arXiv preprint arXiv:1404.1869*.
- Iandola, F. N.; Han, S.; Moskewicz, M. W.; Ashraf, K.; Dally, W. J.; and Keutner, K. 2016. SqueezeNet: AlexNet-level accuracy with 50x fewer parameters and 0.5 MB model size. *arXiv preprint arXiv:1602.07360*.
- Jing, Y.; Yang, Y.; Feng, Z.; Ye, J.; and Song, M. 2017. Neural Style Transfer: A Review. *CoRR* abs/1705.04058. URL <http://arxiv.org/abs/1705.04058>.
- Jing, Y.; Yang, Y.; Feng, Z.; Ye, J.; Yu, Y.; and Song, M. 2019. Neural Style Transfer: A Review. *IEEE Transactions on Visualization and Computer Graphics* 11. ISSN 2160-9306. doi: 10.1109/tvcg.2019.2921336. URL <http://dx.doi.org/10.1109/tvcg.2019.2921336>.
- Johnson, J.; Douze, M.; and Jégou, H. 2019. Billion-scale similarity search with GPUs. *IEEE Transactions on Big Data*.
- Kalantidis, Y.; and Avrithis, Y. 2014. Locally optimized product quantization for approximate nearest neighbor search. In *Proceedings of the IEEE Conference on Computer Vision and Pattern Recognition*, 2321–2328.
- Karras, T.; Aila, T.; Laine, S.; and Lehtinen, J. 2017. Progressive Growing of GANs for Improved Quality, Stability, and Variation.
- Knuth, D. E. 1997. *The art of computer programming*, volume 3. Pearson Education.
- Koch, G.; Zemel, R.; and Salakhutdinov, R. 2015. Siamese neural networks for one-shot image recognition. In *ICML deep learning workshop*, volume 2.
- Le Corbeiller, C. 1974. *China Trade Porcelain: Patterns of Exchange: Additions to the Helena Woolworth McCann Collection in the Metropolitan Museum of Art*. Metropolitan Museum of Art.

- Levy, A. Y.; Mumick, I. S.; and Sagiv, Y. 1994. Query optimization by predicate move-around. In *VLDB*, 96–107.
- Liao, J.; Yao, Y.; Yuan, L.; Hua, G.; and Kang, S. B. 2017. Visual attribute transfer through deep image analogy. *arXiv preprint arXiv:1705.01088*.
- Liao, L.; He, X.; Zhao, B.; Ngo, C.-W.; and Chua, T.-S. 2018. Interpretable multimodal retrieval for fashion products. In *Proceedings of the 26th ACM international conference on Multimedia*, 1571–1579.
- Lin, T.-Y.; Maire, M.; Belongie, S.; Hays, J.; Perona, P.; Ramanan, D.; Dollár, P.; and Zitnick, C. L. 2014. Microsoft coco: Common objects in context. In *European conference on computer vision*, 740–755. Springer.
- Liu, Z.; Luo, P.; Wang, X.; and Tang, X. 2015. Deep Learning Face Attributes in the Wild. In *Proceedings of International Conference on Computer Vision (ICCV)*.
- Lu, P.; Huang, G.; Fu, Y.; Guo, G.; and Lin, H. 2018. Learning Large Euclidean Margin for Sketch-based Image Retrieval. *CoRR* abs/1812.04275. URL <http://arxiv.org/abs/1812.04275>.
- Manning, C. D.; Raghavan, P.; and Schütze, H. 2008. *Introduction to information retrieval*. Cambridge university press.
- Marcel, S.; and Rodriguez, Y. 2010. Torchvision the machine-vision package of torch. In *Proceedings of the 18th ACM international conference on Multimedia*, 1485–1488.
- Marchiori, E. 2009. Class conditional nearest neighbor for large margin instance selection. *IEEE Transactions on Pattern Analysis and Machine Intelligence* 32(2): 364–370.
- McCandless, M.; Hatcher, E.; Gospodnetić, O.; and Gospodnetić, O. 2010. *Lucene in action*, volume 2. Manning Greenwich.
- Mellina, C. 2017. Introducing Similarity Search at Flickr. URL <https://code.flickr.net/2017/03/07/introducing-similarity-search-at-flickr/>.
- Nichol, K. 2016. Painter by numbers, wikiart.
- Olah, C.; Mordvintsev, A.; and Schubert, L. 2017. Feature Visualization. *Distill* doi:10.23915/distill.00007. <https://distill.pub/2017/feature-visualization>.
- Omohundro, S. M. 1989. *Five balltree construction algorithms*. International Computer Science Institute Berkeley.
- Pedregosa, F.; Varoquaux, G.; Gramfort, A.; Michel, V.; Thirion, B.; Grisel, O.; Blondel, M.; Prettenhofer, P.; Weiss, R.; Dubourg, V.; et al. 2011. Scikit-learn: Machine learning in Python. *the Journal of machine Learning research* 12: 2825–2830.
- Plummer, B. A.; Kordas, P.; Hadi Kiapour, M.; Zheng, S.; Piramuthu, R.; and Lazebnik, S. 2018. Conditional image-text embedding networks. In *Proceedings of the European Conference on Computer Vision (ECCV)*, 249–264.
- Sandler, M.; Howard, A. G.; Zhu, M.; Zhmoginov, A.; and Chen, L. 2018. Inverted Residuals and Linear Bottlenecks: Mobile Networks for Classification, Detection and Segmentation. *CoRR* abs/1801.04381. URL <http://arxiv.org/abs/1801.04381>.
- Schroff, F.; Kalenichenko, D.; and Philbin, J. 2015. FaceNet: A Unified Embedding for Face Recognition and Clustering. In *The IEEE Conference on Computer Vision and Pattern Recognition (CVPR)*.
- Traina, C.; Traina, A. J. M.; and de Figuciredo, J. M. 2004. Including conditional operators in content-based image retrieval in large sets of medical exams. In *Proceedings. 17th IEEE Symposium on Computer-Based Medical Systems*, 85–90.
- Veit, A.; Belongie, S.; and Karaletsos, T. 2016. Conditional Similarity Networks.
- Volker, T. 1954. *Porcelain and the Dutch East India Company: as recorded in the Dagb-Registers of Batavia Castle, those of Hirado and Deshima and other contemporary papers; 1602-1682*, volume 11. Brill Archive.
- Wang, J.; Shen, H. T.; Song, J.; and Ji, J. 2014. Hashing for Similarity Search: A Survey. *CoRR* abs/1408.2927. URL <http://arxiv.org/abs/1408.2927>.
- Wang, X. 2011. A fast exact k-nearest neighbors algorithm for high dimensional search using k-means clustering and triangle inequality. In *The 2011 International Joint Conference on Neural Networks*, 1293–1299. IEEE.
- Xie, S.; Girshick, R. B.; Dollár, P.; Tu, Z.; and He, K. 2016. Aggregated Residual Transformations for Deep Neural Networks. *CoRR* abs/1611.05431. URL <http://arxiv.org/abs/1611.05431>.
- Yamins, D. L.; Hong, H.; Cadieu, C. F.; Solomon, E. A.; Seibert, D.; and DiCarlo, J. J. 2014. Performance-optimized hierarchical models predict neural responses in higher visual cortex. *Proceedings of the National Academy of Sciences* 111(23): 8619–8624.
- Yan, D.; Wang, Y.; Wang, J.; Wang, H.; and Li, Z. 2019. K-nearest Neighbors Search by Random Projection Forests. *IEEE Transactions on Big Data*.

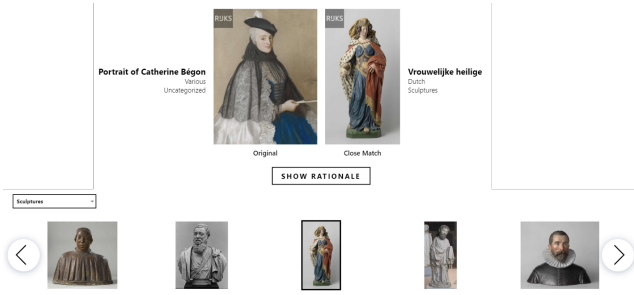


Figure 8: Example of the conditioning abilities of MosAic. The query image (top left) is provided along with a medium conditioner restricts retrieved images to sculptures. Selecting a match from the carousel below brings it up beside the query image for comparison.

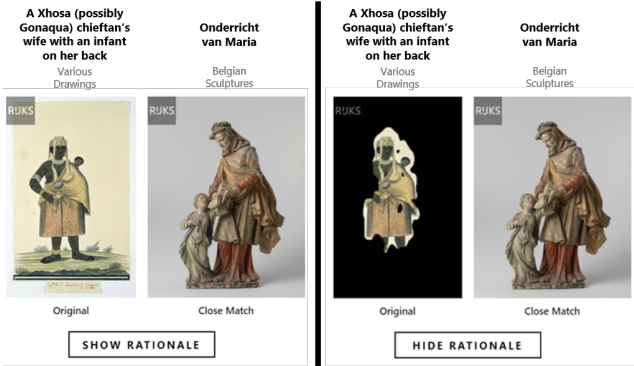


Figure 9: Using SHAP to explain the similarity between the query image and any requested match. Unimportant pixels have been masked. In the example above, the subject of the work is selected as an important contribution to the similarity.

A Website

As an application of CIR for the public, we introduce MosAic (aka.ms/mosaic), a website that allows users to explore art matches conditioned on culture and medium. MosAic’s front-end is built on React (Fedosejev 2015), and its back-end is built on Azure Kubernetes Service and Azure App Services. Figure 8 provides an example of a user query conditioned on the “sculpture” label. This query yields a Dutch sculpture that depicts a female wearing a blue dress and an outer layer across the shoulders, much like the query image. Users can view rows of matched artwork returned for a specific query to see multiple matches for each conditioner. MosAic also leverages SHAP to explain match rationales as in Figure 9 and Azure Search to provide text-based querying in addition to CIR. This allows users find and select specific works from the collection to explore with CIR.

B Visualizing Failure Cases

Figure 10 (a) shows how conditioners that do not share a common support can yield low diversity conditional neighbors. Though sharing a common support is certainly helpful, it is not mandatory as shown by Figure 10 (b). Some potential mitigations for these effects could be to fine tune learned embeddings to promote diverse queries, or to re-weight query outputs based on diversity. Addition-

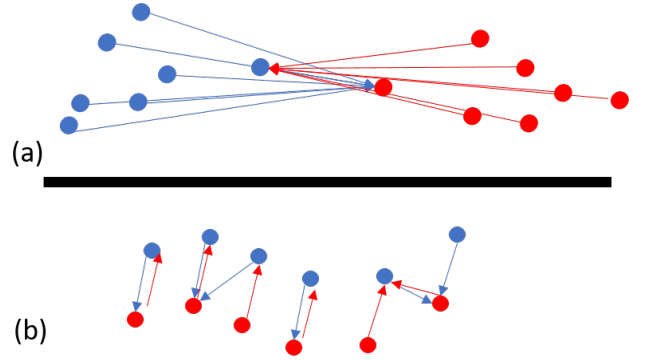


Figure 10: A schematic illustration of how conditional KNN can yield to a lack of diversity in particular geometries. (a) shows how low diversity can occur when there is no overlap of supports. Figure (b) shows how support intersection is not necessary for quality alignment

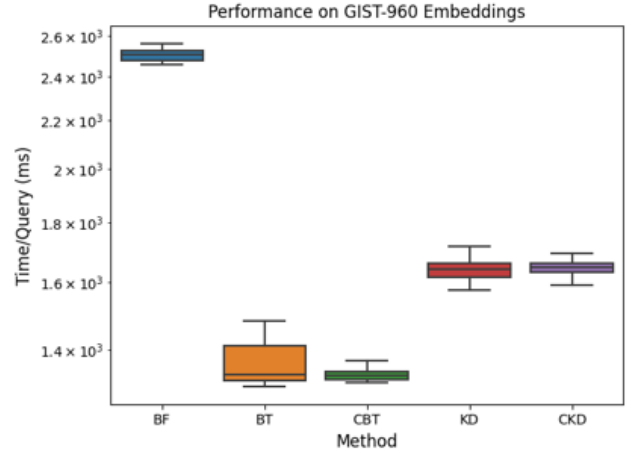


Figure 11: Performance of CKNN in unconditional case when $\mathcal{S} = \mathcal{X}$. Checking the remaining node set does not noticeably affect query time for both KD and Ball Tree (BT) methods. BF represents a Brute Force comparison.

ally, an initial alignment with an optimal transport method could mitigate these effects (Grave, Joulin, and Berthet 2018).

C Evaluating the Overhead of Conditional Retrieval

We find that our CKNN data-structures do not contribute overhead to “unconditional” queries where $\mathcal{S} = \mathcal{X}$. Figure 11 shows a box-plot of query times for unconditional queries on the GIST 960 embeddings, this demonstrate that checking conditioner subsets do not affect the distribution of query times. Table 6 shows this affect on a broad class of large-scale benchmarking datasets with both euclidean and angular distance. For both Figure 11 and Table 6, we use training and testing sets from (Aumüller, Bernhardsson, and Faithfull 2018).

Dataset	CKNN Method		
	KD+R	KD+F	CKD
FMNIST	7+4k	79	23
MNIST	8+4k	75	24
Glove-25	5+8k	126	21
Glove-50	24+15k	284	55
Glove-100	44+20k	523	99
Glove-200	60+40k	1457	133
NYT	14+10k	165	39
SIFT	22+23k	237	63

Table 4: Query times (ms) of KD Tree based KNN methods with random conditions. The KD tree algorithm does not perform as well as the ball tree in high dimensions so all times are slower. However, CKD is still faster than other approaches.

D Conditional KD Trees

Our approach of adding a conditional index to adaptively prune a KNN tree can apply to a variety of KNN algorithms. Another common method is the KD tree, which splits points based on separating hyperplanes. This approach is known to perform better in smaller dimensions (Dasgupta and Freund 2008). In table 4 we explore the performance of KD trees, which generally do not perform as well as Ball Trees on our dataset, but still show the trend that Conditional approaches beat out query-then-filter approaches.

E The Effect of Conditioner Locality

The performance of a conditional KNN system depends on the geometry of the full dataset as well as the conditioners. “Local” conditioners tend to mirror the geometry of the data, and thus are better captured by sub-trees of the original KNN tree. Furthermore, local conditioners increase the odds that a query could be separated from valid points by thousands of invalid points. Table 5 shows these two effects, the performance of conditional methods improve with locality, and the performance of query-then-filter methods dramatically degrade. In this experiment, local subsets were formed by class labels in the MNIST and FMNIST case, and by k-means clusters ($K=10$) in the remaining datasets. Results are averaged across all conditions.

F The Effect of Dimensionality

It is well known that KNN performance depends on the dimensionality of the data, as well as the *intrinsic* dimensionality of the data manifold (Dasgupta and Freund 2008). In Figure 12 we show these effects on the MNIST dataset. Acceleration due to KNN trees dramatically improves in lower dimensions.

G Additional Matches

In addition to the matches displayed in Figure 5 we provide several additional results. Figure 13 shows additional matches for a single query, and Figure 14 shows matches across several different queries. Figure 15 shows random matches to give a sense of the method’s average-case results.

Dataset	CKNN Method				
	BF	BT+F	LOPQ+F	BT+R	CBT
FMNIST	7	208	122	6 + 3k	8
MNIST	7	177	41	6 + 3k	9
Glove-25	29	463	296	6 + 7k	22
Glove-50	43	649	327	22 + 11k	35
Glove-100	68	1072	404	40 + 17k	60
Glove-200	129	1673	1429	45 + 32k	79
NYT	30	220	110	12 + 8k	21
SIFT	70	1473	1064	28 + 20k	47

Table 5: Query times (ms) of Conditional KNN methods across several benchmarking datasets from (Aumüller, Bernhardsson, and Faithfull 2018) with local conditioners formed from either class labels (FMNIST + MNIST) or k-means ($k=10$) clusters. Our conditional method, CBT, outperforms other approaches including those most commonly used in production search engines, LPQ+F. Furthermore, Query-then-filter approaches perform significantly worse when queries have local structure. Please see the Section 3.2 for method details.

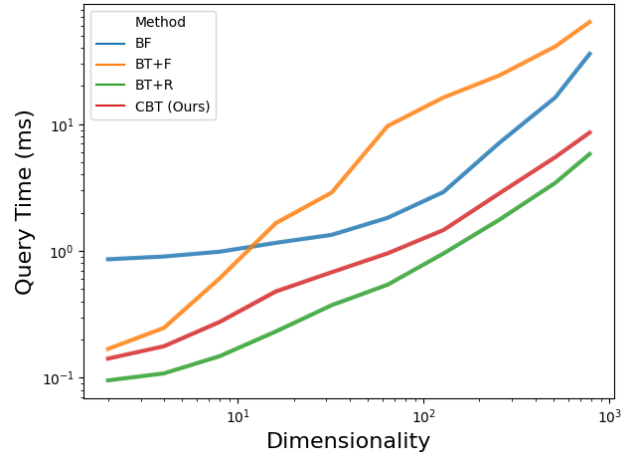


Figure 12: Query time vs dataset dimensionality for MNIST CKNN Task with random conditioners. Tree based methods perform better relative to brute force at lower dimensions



Figure 13: Additional conditional image retrieval results on artworks from the Metropolitan Museum of Art and Rijksmuseum using media (top row text) and culture (bottom row text) as conditioners.



Figure 14: Additional conditional image retrieval results on artworks from the Metropolitan Museum of Art and Rijksmuseum using top row text as conditioners.

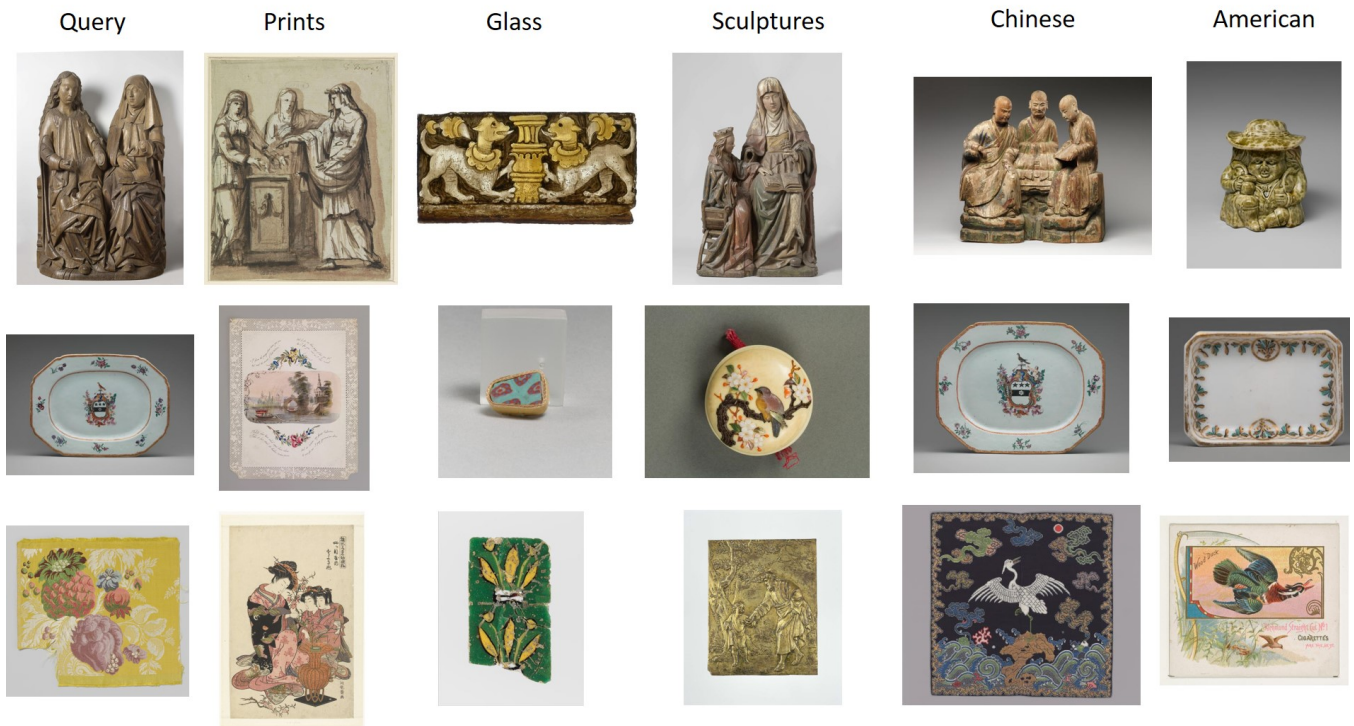


Figure 15: Randomly selected conditional image retrieval results on artworks from the Metropolitan Museum of Art and Rijksmuseum using top row text as conditioners.

Dataset	Size	Dim	Metric	Method					
				BF	BT	CBT	KD	CKD	Annoy
FMNIST	60,000	784	E	122 ± 3	62 ± 2	62 ± 2	67 ± 8	68 ± 8	14 ± 3
GIST	1,000,000	960	A	2511 ± 58	1375 ± 89	1330 ± 14	1618 ± 276	1599 ± 256	45 ± 14
Glove	1,183,514	100	A	446 ± 9	415 ± 7	441 ± 9	447 ± 22	473 ± 21	17 ± 2
Glove	1,183,514	200	A	745 ± 9	454 ± 11	613 ± 11	530 ± 11	682 ± 10	20 ± 3
Glove	1,183,514	25	A	232 ± 8	145 ± 17	147 ± 17	64 ± 38	67 ± 38	12 ± 1
Glove	1,183,514	50	A	316 ± 6	240 ± 5	246 ± 5	246 ± 34	252 ± 34	14 ± 1
MNIST	60,000	784	E	121 ± 2	63 ± 2	63 ± 1	68 ± 15	68 ± 15	18 ± 2
NYT	290,000	256	A	215 ± 3	115 ± 13	120 ± 13	108 ± 59	112 ± 61	20 ± 1
SIFT	1,000,000	128	E	436 ± 4	192 ± 37	270 ± 51	146 ± 59	190 ± 77	13 ± 1

Table 6: Unconditional benchmarking results on reference datasets from (Aumüller, Bernhardsson, and Faithfull 2018). Results show that our approach does not introduce overheads in the unconditional setting and can be used to broaden the family of KNN operations without sacrificing speed. We include a single approximate KNN approach, Annoy, to allow for comparison between our exact KNN baselines, and a widely used approximate KNN method. Metric “A” and “E” represent angular and euclidean distance respectively.